

# Microstructure and Mechanical Properties Determined in Compressive Tests of Quasi-Rapidly Solidified NiAl-Cr(Mo)-Hf Eutectic Alloy After Hot Isostatic Pressure and High Temperature Treatments

L.Y. Sheng, L. Nan, W. Zhang, J.T. Guo, and H.Q. Ye

(Submitted November 14, 2008; in revised form June 16, 2009)

The effect of high cooling rate of approximately  $10^2$  K/s and subsequent hot isostatic pressure (HIP) and high temperature (HT) treatment on the microstructure and mechanical properties of NiAl-based intermetallic alloys was investigated. The results reveal that rapid solidification refines the microstructure of the NiAl-Cr(Mo)-0.5Hf eutectic alloy and transforms the  $\text{Ni}_2\text{AlHf}$  Heusler phase, which is present in the equilibrium state to a metastable Hf(Ni, Al, Cr) solid solution phase. Simultaneously, the shape and distribution of the Hf(Ni, Al, Cr) solid solution phase were considerably improved. After the HIP treatment, the Hf(Ni, Al, Cr) solid solution phase has changed from continuous distribution along eutectic cell boundaries into semicontinuous distribution, and the primary NiAl(Cr, Mo) phase has coarsened. The HT treatment reduces the volume fraction of the primary NiAl(Cr, Mo) phase and optimizes the distribution of the Hf(Ni, Al, Cr) solid solution phase. Rapid solidification and the resulting fine-grained microstructure will significantly improve the mechanical properties of the alloy in compression tests. However, additional HIP and HT treatments enhance the high-temperature strength properties obviously.

**Keywords** mechanical property, microstructure, NiAl-Cr(Mo)-Hf eutectic alloy, rapid solidification

## 1. Introduction

As potential high-temperature structural materials, NiAl owns many advantages compared to nickel-based superalloys such as high melting point, low density, excellent oxidation resistance as well as high thermal conductivity. However, the limited room temperature (RT) ductility and fracture toughness as well as the poor elevated temperature strength and creep resistance seriously will hinder its commercial applications (Ref 1-3). Previous investigations on NiAl-based alloys show that the addition of refractory metals like V, Mo, Cr, and Re can improve their RT fracture toughness and elevated temperature strength by performing directional solidification of the quasi-binary or ternary eutectic systems (Ref 4-7). Among NiAl-based eutectic alloys, Ni-33Al-28Cr-6Mo [NiAl-Cr(Mo) for short] has been regarded as one of the most appropriate choices because of its optimal good combination of elevated temperature strength, high elastic stiffness, and RT fracture toughness

(Ref 8, 9). Recent studies (Ref 10, 11) showed that a small amount of Hf addition can well improve the high temperature strength of the NiAl-Cr(Mo) alloy, but the addition of Hf leads to the decrease in the RT ductility and fracture toughness, which can be attributed mainly to the segregation of Hf on phase and eutectic cell boundaries. Therefore, it is believed that the mechanical properties of the alloy can be improved by a homogeneous distribution and optimal morphology of the Hf-rich phase. Also the investigations (Ref 12, 13) on strong magnetic field-treated alloys already revealed that the improvement on the distribution and morphology of the Hf-rich phase might increase the mechanical properties of the alloy. However, the electromagnetic equipment for providing a strong magnetic field treatment limits its application. Nevertheless, rapid solidification is a suitable technique that can be utilized to achieve optimum properties of NiAl(Cr, Mo) alloys because it will prevent the segregation of elements, refine the microstructure, and also extend the solid solubility. Previous studies (Ref 14, 15) have proved that rapid solidification is very effective to improve the morphology of the precipitates in phase or eutectic cell boundaries and refine the microstructure in general. In this study, the microstructure and mechanical properties achieved in compression tests of rapidly solidified (RS) NiAl-Cr(Mo)-Hf eutectic alloy and the effect of hot isostatic pressure (HIP) and high temperature (HT) treatments were investigated.

L.Y. Sheng, Institute of Industry Technology, Guangzhou & Chinese Academy of Sciences, Guangzhou 511458, China and Institute of Metal Research, Chinese Academy of Sciences, Shenyang 110016, China; and L. Nan, W. Zhang, J.T. Guo, and H.Q. Ye, Institute of Metal Research, Chinese Academy of Sciences, Shenyang 110016, China. Contact e-mail: lysheng@ymail.com.

## 2. Experimental Procedure

The investigated alloy, Ni-33Al-28Cr-5.7Mo-0.3Hf (at.%) [NiAl-Cr(Mo)-Hf for short], was prepared by induction melting

using the as starting materials of 99.99% Ni, 99.9% Al, 99.9% Cr, 99.9% Mo, and 99.9% Hf, respectively. The melted alloy was cast into rods with 24 mm in diameter. These rods fabricated by conventional casting technique were cut into slices. Some of them were investigated in the as-cast state, and the remaining ones were crushed for subsequent rapid solidification experiment. The rapid solidification was conducted with water-cooled copper mold method, which has significant undercooling capacity. First, an appropriate amount of the alloy was melted again in quartz crucible in high vacuum with argon atmosphere. Then the remelted alloy was injected through a nozzle into a copper mold by argon with high speed about 200 m/s. The copper mold has inner cavity with a size of  $\varnothing$  5 mm  $\times$  80 mm and is cooled by high-speed water. The RS samples were divided into three groups. One group is the RS state; the other group was treated at high temperatures of about 1623 K for 24 h followed by furnace cooling; and the third group was treated by HIP treatment of 150 MPa/1473 K/3 h.

Microstructural characterization of the different samples was carried out by using S-3400 scanning electron microscope (SEM) equipped with an energy dispersive spectrometry (EDS) and the compositions of the constituent phases were detected by EPMA-1610 electron probe microanalysis (EPMA). The foils for transmission electron microscopic (TEM) observation were prepared by using the conventional twin jet polishing technique applying an electrolyte of 10% perchloric acid in methanol at  $-20$  °C after mechanical polishing to 50  $\mu$ m and cutting disc to 3.0 mm in diameter. The TEM investigation was performed by using a JEM-2010 transmission electron microscope operated at 200 kV.

The test specimens with the size of 4 mm  $\times$  4 mm  $\times$  6 mm for evaluating the mechanical properties in compressions were cut from different processed alloys by electrodischarge machining. The surfaces were mechanically ground with 600-grit SiC

abrasive prior to compression test. The compression tests were conducted using a computer servo-controlled Gleeble-1500 testing machine at RT and at 1273 K, by applying an initial strain rate of  $1 \times 10^{-3} \text{ s}^{-1}$ . The compressive specimen was resistance heated to deformation temperature at a heating rate of  $10$  °C/s and held at that temperature for 120 s by thermo-coupled-feedback-controlled AC current before compression. The specimens at 1273 K were deformed to half of their original height and water quenched immediately.

### 3. Results and Discussion

#### 3.1 Microstructural Characteristics

Typical SEM images of the conventionally cast (CC) NiAl-Cr(Mo)-Hf alloy are shown in Fig. 1(a) and (b). The alloy is composed of eutectic cells, coarse NiAl dendrites, and the Hf-rich phase, which is mainly distributed on the cell boundaries. The eutectic cells consist of black shining NiAl and gray apparent Cr(Mo) platelets forming a radially emanating pattern from the cell interior to its boundaries. The interlamellar spacing of NiAl and Cr(Mo) platelets near the cell center is finer than that at the periphery of the cells. Coarser Cr(Mo) rods, primary NiAl(Cr,Mo) phase, and white Hf-rich phase mainly distribute within the intercellular zones. Moreover, there are still primary NiAl(Cr,Mo) solid solution crystals which have been formed in eutectic cells. SEM observations on the Hf-rich phases reveal that there are two different Hf phases present in the CC alloy. EDS analysis reveals that one kind of Hf phase possesses almost 70 at.% Hf, while the other one exhibits only 20 at.% Hf. TEM analyses of the Hf-rich phases confirm these observations, as shown in Fig. 1(c) and (d).

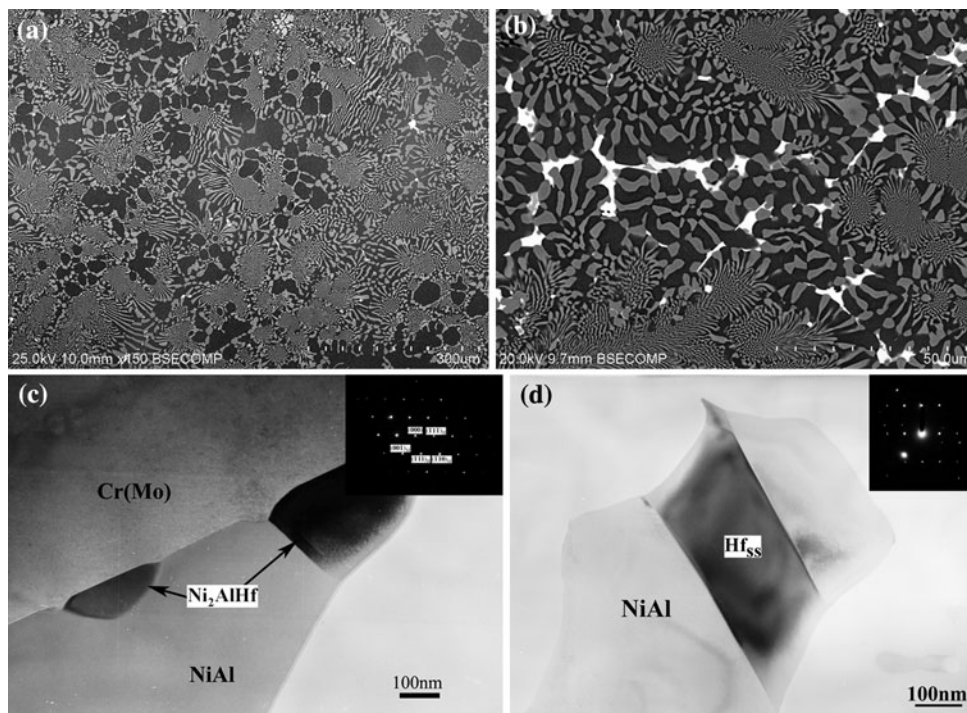


**Fig. 1** SEM micrographs exhibit the microstructures of as cast NiAl-Cr(Mo)-Hf eutectic alloy. (a) Low magnification, (b) high magnification, (c) TEM bright field image showing Ni<sub>2</sub>AlHf particles, and (d) TEM bright field image revealing the Hf solid solution phase

One Hf phase was detected as the Ni<sub>2</sub>AlHf Heusler phase, which possesses the L<sub>21</sub> crystal structure. Former investigations (Ref 11) revealed that the Heusler phase has the orientation relationship with the NiAl matrix like [111]<sub>NiAl</sub> // [111]<sub>Heusler</sub> and (10 $\bar{1}$ )<sub>NiAl</sub> // (20 $\bar{2}$ )<sub>Heusler</sub>. It is confirmed that the other phase is an Hf solid solution, which exhibits a hexagonal crystal structure. However, the Hf solid solution phase represents only a small amount of the Hf-rich phases.

The typical microstructure of the rapidly solidified NiAl-Cr(Mo)-Hf alloy is shown in Fig. 2(a) and (b). Apparently, the microstructure of the RS alloy is quite different from that of CC alloy as a result of the applied high cooling rate. The average eutectic cell size in an RS alloy of about 20 to 30  $\mu$ m is smaller than that of CC alloy. The interlamellar spacing ( $\lambda$ ) of the coexisting phases in eutectic cell interior of the RS alloy is finer than that of the CC alloy, ranging from 5.62 to 0.39  $\mu$ m, respectively. The width of the intercellular region of 1 to 2  $\mu$ m of the RS alloy is smaller than 10 to 30  $\mu$ m in the CC alloy. The primary NiAl(Cr,Mo) solid solution crystals in the RS alloy with an average size of 15  $\mu$ m are distributed at the eutectic cell interior or on cell boundary. By comparing Fig. 1(a) with Fig. 2(a), it is observed that the Ni<sub>2</sub>AlHf phase has been distinctly refined and evenly distributes on the eutectic cell boundaries.

TEM observations on the RS alloy samples show that there frequently appear interface dislocation networks at the interfaces of NiAl(Cr,Mo) and Cr(Mo) phases, as shown in Fig. 2(c). Such a high density of interface dislocation networks demonstrates the extended of solid solubility. As shown in Table 1, in the RS alloy, the amount of Ni and Al solutes in the Cr(Mo) phase is higher than that of Cr and Mo in the NiAl phase. There is no doubt that this will increase the difference in the lattice parameters between the NiAl(Cr, Mo) and Cr(Mo,

Ni, Al) phases, which will result in high misfit interface dislocations density at the NiAl(Cr, Mo) and Cr(Mo, Ni, Al) phases boundaries. According to the result of Probst-Hein et al. (Ref 16), this high density of misfit interface dislocations might be beneficial to improve the strength of the RS alloy. In addition, a large amount of fine NiAl particles precipitate out in the Cr(Mo, Ni, Al) phase with an average size of 20 nm, which also demonstrates that the high cooling rate inhibits the diffusivity of coexisting components. However, in the primary NiAl(Cr, Mo) solid solution, there are some fine Cr(Mo) particles precipitating out with several decade of nanometers in size, as shown in Fig. 2(c). This exhibits an extended solid solubility of the coexisting metallic elements during rapid solidification.

The EPMA results of the NiAl(Cr, Mo) and Cr(Mo, Ni, Al) phases in the CC and RS alloys are enumerated in Table 1. For the RS alloy, the solubility of Cr and Mo in the primary NiAl(Cr, Mo) phase, Ni, Al in Cr(Mo) phase are higher than that in the CC alloy. As shown in Table 1, an amount of 7.47 at.% Cr was detected in the primary solidified

**Table 1 Compositions of the coexisting NiAl(Cr,Mo,Hf) and Cr(Mo,Ni,Al) phases in the conventionally cast (CC) and rapidly solidified (RS) NiAl-Cr(Mo)-Hf alloys**

Alloy	Phase	Compositions, at.%				
		Ni	Al	Cr	Mo	Hf
CC	NiAl(Cr,Mo,Hf)	46.33	49.76	3.65	0.07	0.19
	Cr(Mo,Ni,Al)	6.96	5.50	71.05	16.49	...
RS	NiAl(Cr,Mo,Hf)	47.60	45.28	6.68	0.12	0.32
	Cr(Mo,Ni,Al)	10.98	9.49	64.95	14.58	...

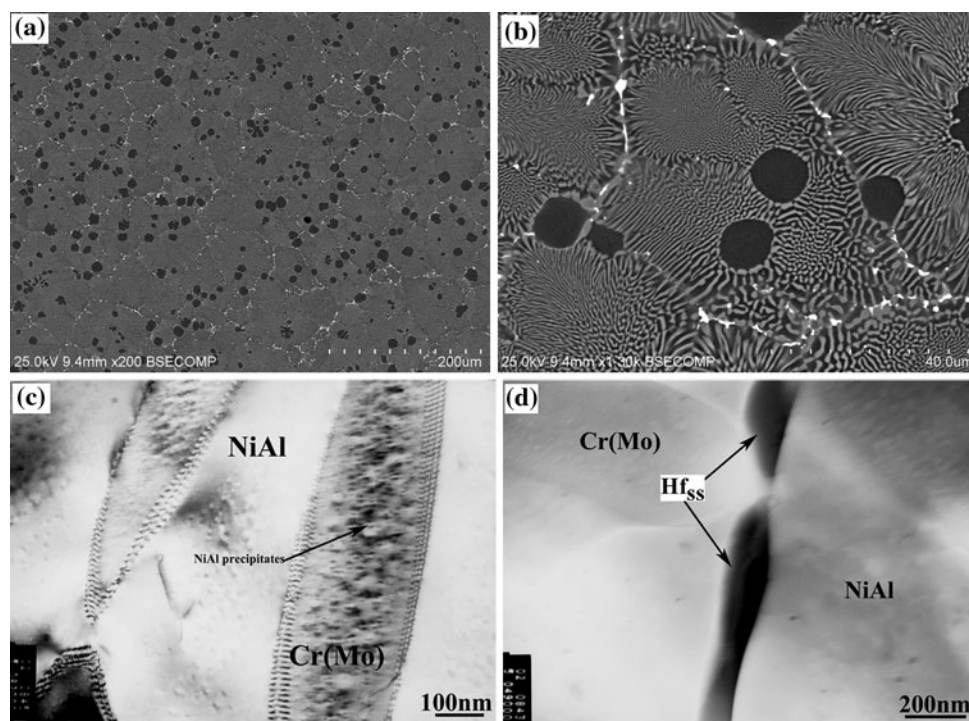


**Fig. 2** SEM and TEM images presenting the characteristic microstructures of rapidly solidified NiAl-Cr(Mo)-Hf alloy. (a) Low magnification, (b) high magnification, (c) TEM BF micrograph exhibiting NiAl and Cr(Mo) lamellar, and (d) TEM BF image of Hf solid solution



NiAl(Cr, Mo) phase of the RS alloy by EPMA, which is more than its solid solubility in the equilibrium solidification state (Ref 17).

### 3.2 Microstructure Features of the RS Alloy After HIP and HT Treatments

The microstructure of the RS NiAl-Cr(Mo)-Hf alloy after HIP and HT treatments is shown in Fig. 3(a) and (b). The as-HIP-treated RS alloy (RS-HIP) reveals a slightly coarsened microstructure. Especially, the primary NiAl(Cr, Mo) phase in the as-RS-HIP state exhibits a change from the spherical to the polyhedral shape. The NiAl(Cr, Mo) and Cr(Mo, Ni, Al) phases on the eutectic cell boundary show also a slight coarsening. However, the Hf-rich phases on the eutectic cell boundaries are refined and discontinuously distributed. Different from the RS-HIP alloy, the primary NiAl(Cr, Mo) phases in the HT-treated RS alloy (RS-HT) have not been coarsened at all, but there are many coarse Cr(Mo) particles precipitating out in the primary NiAl(Cr, Mo) solid solution phase. Compared with the RS-HIP alloy, the RS-HT alloy possesses more fine Hf-rich particles, and the volume portion of the Hf-rich phase decreases.

TEM observations on the RS-HIP or RS-HT alloy show that the Hf-rich phases are mostly Hf solid solutions, especially on

the eutectic cell boundaries. Only a small portion of the Hf phases consist of the Ni<sub>2</sub>AlHf phases, which is mainly distributed along the NiAl(Cr, Mo) and Cr(Mo) interfaces of the eutectic cells. In addition, some small Hf solid solution particles were detected on NiAl(Cr, Mo) and Cr(Mo) interphases, as shown in Fig. 4(a). Comparatively, the amount and the size of the Hf-rich phase in the RS-HT alloy are smaller than those of the Hf-rich phase in the RS-HIP alloy. As is well known, the Hf solid solution phase has better ductility than the Ni<sub>2</sub>AlHf phase. Therefore, the precipitates of Hf solid solution phases and the optimization of distribution and morphology Hf solid solution and Ni<sub>2</sub>AlHf particles will contribute to the improvement of the mechanical properties of the alloy. Moreover, some HfO<sub>2</sub> oxide particles were detected in the RS-HT alloy. Such kind of oxide maybe formed during conventional castings. However, the HT treatment results in a segregation of the small oxide particles.

### 3.3 Mechanical Properties

The mechanical data determined in compression test at RT and at 1273 K of the investigated alloy in different states is shown in Table 2. It is obvious that compared with the CC alloy, the compressive properties of the RS alloy at RT are improved significantly, but at 1273 K, the compressive

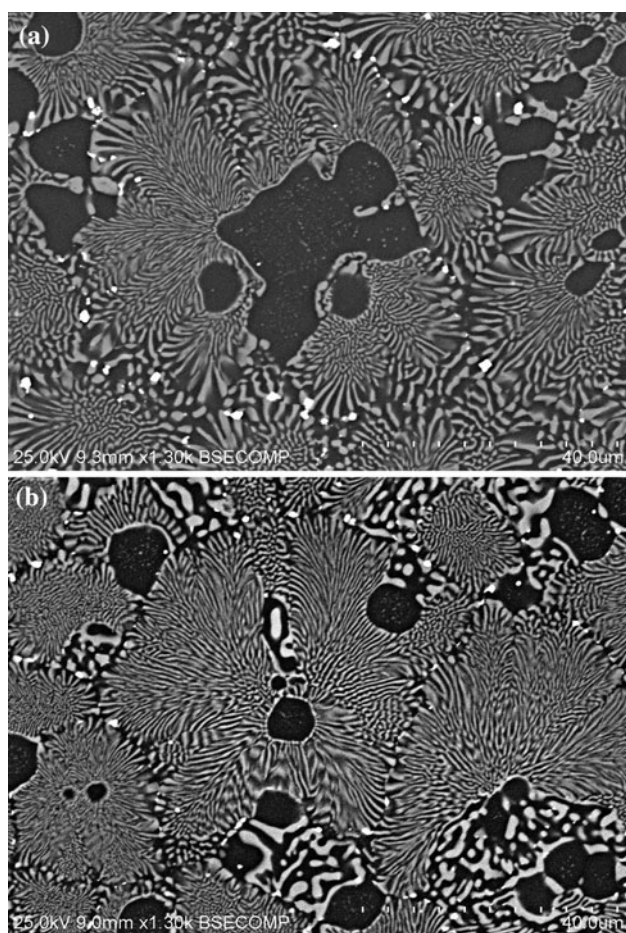


**Fig. 3** SEM micrograph shows the microstructure of the rapidly solidified NiAl-Cr(Mo)-Hf alloys after HIP and HT treatments. (a) RS-HIP-processed alloy and (b) RS-HT-conditioned alloy

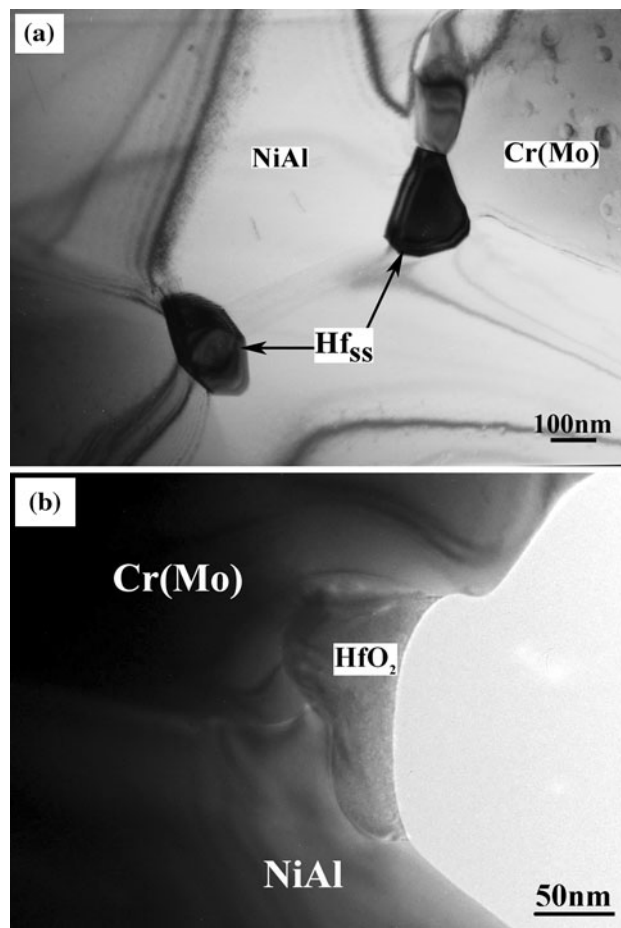


**Fig. 4** Different precipitates in the rapidly solidified NiAl-Cr(Mo)-Hf alloys after HIP and HT treatments. (a) TEM BF micrograph indicating Hf solid solution particles in the RS-HIP alloy and (b) TEM BF image showing a Hf oxide particle in the RS-HT alloy

**Table 2 Mechanical properties of the investigated alloys deformed in compressive tests at RT and 1273 K**

Alloys	Test temperature	Yield strength, MPa	Compressive strength, MPa	Compressive strain, %
CC	RT	1125	1575	7
	1273 K	330	420	>25
RS	RT	1423	2045	17
	1273 K	390	430	>25
RS-HIP	RT	1330	1920	24
	1273 K	510	565	>25
RS-HT	RT	1250	1800	19
	1273 K	450	490	>25

properties increase only a little. For the RS NiAl-Cr(Mo)-Hf alloy, the extended solid solution of the alloying elements in NiAl(Cr, Mo) and in Cr(Mo) phase, the large volume fraction of the eutectic cells, the fine lamellar spacing, and the optimization of the Hf solid solution and Ni<sub>2</sub>AlHf phases all beneficially improve the mechanical properties of the RS alloy at RT and at 1273 K. However, there is a small increase in the elevated temperature strength compared with the CC alloy. The reason for this is the weak intercellular zones and the large amount of primary NiAl(Cr, Mo) phase. For the lamellar eutectic NiAl-Cr(Mo)-Hf alloy, cracks easily propagate along the cell boundary when a stress is applied to the eutectic alloy due to the coarser NiAl/Cr(Mo) platelets and the primary NiAl(Cr, Mo) phase at intercellular zone. However, rapid solidification process produces more cell boundaries, because of the eutectic cell refinement, which becomes the dominant factor in determining the high temperature strength. At 1273 K, the strength of NiAl is lower than that of the eutectic cell and Cr(Mo) phase. In as RS alloy, the NiAl(Cr, Mo) phase will yield at first, during high temperature deformation. It is concluded that the strengthening effect due to dislocations networks and effective solid solution is partly compensated by the weakening effect of the cell boundaries and large amounts of primary NiAl(Cr, Mo) phases. The transformation of Hf solid solution particles might be another factor that leads to the small increase in the compressive strength at 1273 K.

After HIP and HT treatments, the compressive properties of the RS alloy decrease at RT a little, but increase at 1273 K, especially in the as RS-HIP alloy. Although the precipitates Cr(Mo) in the NiAl phase and NiAl in the Cr(Mo) phase are not so effective for improving the high temperature strength, an optimal distribution and the morphology of the Hf solid solution and Ni<sub>2</sub>AlHf phases will contribute more efficiently to the high temperature strength. Due to the coarsening of the Cr(Mo) phases close to the eutectic cell boundaries and the formation of HfO<sub>2</sub> particles in the RS-HT alloy, the high temperature strength increase is relatively small.

## 4. Conclusions

1. The rapid solidification process refines the eutectic cells and the NiAl and Cr(Mo) lamellar structure effectively and extends the solid solubility of NiAl(Cr, Mo) and Cr(Mo) phases. In addition, most of the Heusler phases transform to the Hf solid solution phases and the

distribution and morphology of Heusler and Hf solid solution phases will be optimized.

2. After HIP treatment, the primary NiAl(Cr, Mo) solid solution phase in the RS alloy exhibits coarsening and the Heusler and Hf solid solution phases are distributed discontinuously on the eutectic cell boundaries.
3. After HT treatment, the amount of primary NiAl(Cr, Mo) phases decreases a little, and coarse Cr(Mo) particles precipitated out in the NiAl solid solution phase. Additionally, some Cr(Mo) lamellae near the eutectic cell boundaries exhibit coarsening.
4. The rapid solidification process improves the mechanical properties of the alloy in compressive tests significantly. Moreover, the HIP and HT treatments improve the compressive properties of the alloy at RT and the compressive strength at 1273 K, respectively.

## References

1. D.B. Miracle, Overview No 104. The Physical and Mechanical Properties of NiAl, *Acta Metall. Mater.*, 1993, **41**(3), p 649–684
2. R.D. Noebe and R.R. Bowman, Physical and Mechanical Properties of the B2 Compound NiAl, *Int. Mater. Rev.*, 1993, **38**(4), p 193–232
3. J.T. Guo, *Ordered Intermetallic Compound NiAl Alloy*, Science Press, Beijing, 2003, p 105–120
4. A. Misra and R. Gibala, Plasticity in Multiphase Intermetallics, *Intermetallics*, 2000, **8**(9–11), p 1025–1034
5. H.E. Cline and J.L. Walter, The Effect of Alloy Additions on the Rod-Plate Transition in the Eutectic NiAl-Cr, *Metall. Trans.*, 1970, **1**, p 2907–2917
6. G. Frommeyer and R. Rablbauer, Defect Properties and Related Phenomena in Intermetallic Alloys, *MRS Symp. Proc.*, Vol. 753, E.P. George, H. Inui, M.J. Mills, and G. Eggeler, Ed., Warrendale, PA, 2003, p 193–208
7. R. Fischer, G. Frommeyer, and A. Schneider, APFIM Investigations on Site Preferences Superdislocations, and Antiphase Boundaries in NiAl(Cr) with B2 Superlattice Structure, *Mater. Sci. Eng. A*, 2003, **353**(1–2), p 87–91
8. X.F. Chen, D.R. Johnson, R.D. Noebe, and B.F. Oliver, Deformation and Fracture of a Directionally Solidified NiAl-28Cr-6Mo Eutectic Alloy, *J. Mater. Res.*, 1995, **10**(5), p 1159–1170
9. J.M. Yang, S.M. Jeng, K. Bain, and R.A. Amato, Microstructure and Mechanical Behavior of In Situ Directional Solidified NiAl/Cr(Mo) Eutectic Composite, *Acta Mater.*, 1997, **45**(1), p 295–308
10. J.T. Guo, C.Y. Cui, Y.H. Qi, and H.Q. Ye, Microstructure and Elevated Temperature Mechanical Behavior of Cast NiAl-Cr(Mo) Alloyed with Hf, *J. Alloys Compd.*, 2002, **343**(1–2), p 142–150
11. J.T. Guo, L.Y. Sheng, Y.X. Tian, L.Z. Zhou, and H.Q. Ye, Effect of Ho on the Microstructure and Compressive Properties of NiAl-Based Eutectic Alloy, *Mater. Lett.*, 2008, **62**(23), p 3910–3912
12. L.Y. Sheng, J.T. Guo, Y.X. Tian, L.Z. Zhou, and H.Q. Ye, The Effect of High Magnetic Field Treatment on the Microstructure and Mechanical Properties of NiAl-Cr(Mo)-02Hf Eutectic alloy, *Acta Metall. Sin.*, 2008, **44**(5), p 524–528 (in Chinese)
13. L.Y. Sheng, J.T. Guo, L.Z. Zhou, and H.Q. Ye, The Effect of Strong Magnetic Field Treatment on Microstructure Room Temperature Compressive Properties of NiAl-Cr(Mo)-Hf Eutectic Alloy, *Mater. Sci. Eng. A*, 2009, **500**(1–2), p 238–243
14. L.Y. Sheng, J.T. Guo, and H.Q. Ye, Microstructure and Mechanical Properties of NiAl-Cr(Mo)/Nb Eutectic Alloy Prepared by Injection-Casting, *Mater. Des.*, 2009, **30**(4), p 964–969
15. L.Y. Sheng, J.T. Guo, L.Z. Zhou, and H.Q. Ye, Microstructure and Mechanical Properties of Rapidly Solidified NiAl-Cr(Mo) Eutectic Alloy Doped with Trace Dy, *J. Alloys Compd.*, 2009, **475**(1–2), p 730–734
16. M. Probst-Hein, A. Dlouhy, and G. Eggeler, Interface Dislocations in Superalloy Single Crystals, *Acta Mater.*, 1999, **47**(8), p 2497–2510
17. T.B. Massalski, *Handbook of Ternary Diagrams*, ASM International, Materials Park, OH, 1995, p 1250–1255